

Molecular Dynamics Study of a Membrane–Water Interface[†]

Feng Zhou and Klaus Schulten*

Department of Biophysics, Department of Physics, and Beckman Institute, University of Illinois at Urbana–Champaign, Urbana, Illinois 61801

Received: July 25, 1994; In Final Form: November 11, 1994[Ⓢ]

A 200 ps molecular dynamics simulation of a membrane bilayer consisting of 202 dilauroylphosphatidylethanolamine molecules and 8108 water molecules at 315 K is conducted. Distribution functions of lipid groups, order parameters, and other properties of the lipid bilayer are calculated and compared with experimental measurements. A detailed analysis is conducted for the structure at the membrane–water interface. Water polarization profile, membrane dipole potential profile, and susceptibility profile are calculated. Simulation results suggest that the polarization of water is determined mainly by the distribution of lipid head groups in the interfacial region. The membrane dipole potential is mainly due to the ester groups linked to the glycerol backbone, while the contribution due to the phosphatidylethanolamine head groups is almost completely cancelled by the contribution due to oriented water molecules. The susceptibility profile suggests a dielectric constant around 30 for the head group–water interface and a dielectric constant around 10 for the ester group region. The ammonium groups of the DLPE membrane are found to form hydrogen bonds with water molecules, while no orientational preference is observed for water molecules around the choline groups of a previously simulated POPC (1-palmitoyl-2-oleoyl-*sn*-glycerol-3-phosphatidylcholine) membrane. Correlations of the membrane surface charge density are also analyzed. The simulations which involved 32 808 atoms included Coulombic forces between all atom pairs evaluated by means of the fast multipole algorithm. Effects of cutting off Coulombic forces at a distance of 8 Å are discussed.

Introduction

Biological membranes have become the subject of intensive modeling studies in recent years.^{1,2} Biological membranes are complex molecular assemblies formed by amphiphilic lipid molecules, membrane proteins, and other molecules like cholesterol and water. Many important biological processes, such as the reactions in the respiratory chain, the photosynthetic reaction, and cell signalling and transport, take place on or across biological membranes and are inherently related to properties of membranes. Obtaining a more detailed and complete understanding of the structure, dynamics, and function of the membrane–water system remains a major task for biophysicists,^{3–6} and one can expect that molecular dynamics simulations can contribute very well in this respect. However, modeling of membrane–water systems involves large system sizes and requires long time simulations. The rotational motion of lipid along its long axis and the *trans/gauche* isomerizations occur in the time range of 100 ps to nanoseconds,^{7–10} collective motion of the membrane hydrocarbon tails occurs on an even longer time scale.¹¹ In addition, a membrane patch large enough to preserve bulk properties, or a membrane patch complexed with a protein of medium size, involves 20 000 atoms or more and a correspondingly large simulation.¹² Such large scale and long time simulations were unachievable until recently due to limitations in computational power. The availability of very efficient algorithms for the evaluation of Coulombic forces¹³ has made it possible to carry out the necessary computations today.

Earlier theoretical models by Marčelja used mean field descriptions to represent the influence of neighboring lipid atoms.¹⁴ Monte Carlo simulations were later used to study the

hydrocarbon regions and the phase transitions of lipid membranes^{15,16} and membrane–cholesterol interactions.^{17,18} Combining the Marčelja mean field model and Brownian dynamics, Pastor *et al.* carried out simulations on a few lipid molecules in the time range of microseconds and reproduced some experimental data.^{19,20} Simulation using detailed atomic models and molecular dynamics techniques on membrane–water systems was pioneered by Berendsen *et al.* on a decanoate (2×16 molecules) membrane²¹ and was later extended to bigger membrane patches including explicit water molecules.^{22,23} Studies on other membrane bilayers such as DLPE (1,2-dilauryl-*sn*-glycerol-3-phosphatidylethanolamine)^{24,25} and DPPC (1,2-dipalmitoyl-*sn*-glycerol-3-phosphatidylcholine)^{26–28} have been carried out in recent years. With the help of newly developed supercomputers, very long simulations on membranes (2 ns for DMPC (1,2-dimyristol-*sn*-glycerol-3-phosphatidylcholine)²⁹) and simulations for very large systems (up to 200 POPC (1-palmitoyl-2-oleoyl-*sn*-glycerol-3-phosphatidylcholine) lipid molecules¹²) have been carried out. These studies have allowed direct comparison with experiments and suggest that MD simulations have become a powerful tool in membrane research and for membrane-related biological processes.

Among the head groups of the lipid molecules found in biological membranes, phosphatidylcholine (PC) and phosphatidylethanolamine (PE) are quite common. Pure lipid membranes, such as the PC or PE membranes, usually undergo a phase transition from the gel (L_{β}) phase to the liquid crystal (L_{α}) phase at a temperature between -20 and 80 °C. Biological membranes generally exist in the liquid crystal phase *in vivo*, and this phase is probably most relevant for most membrane processes. The crystal phase structures of a few membranes, such as that of the DLPE^{30,31} and of the DMPC³² membrane, are known through X-ray crystallography. Even though in the liquid crystal phase the structures are disordered, the X-ray structures do provide some important information on lipid packing in membranes. Differences are observed between the

* To whom correspondence should be sent.

[†] This work was supported by a grant from the National Institutes of Health (P41RRO5969) and by a grant from the National Science Foundation (ASC93-18159).

[Ⓢ] Abstract published in *Advance ACS Abstracts*, January 1, 1995.

DLPE and DMPC membranes: for example, a direct hydrogen-bonding network is observed between neighboring lipid head groups in the DLPE membrane. Compared to PC membranes, PE membranes usually have smaller surface areas per lipid,³³ lower phase transition temperatures,¹ and weaker hydration, i.e., a faster decay in the hydration force.³⁴ Extensive experimental studies have been carried out on PC membranes (particularly DPPC), and simulation studies have been carried out by many researchers.^{12,26,27} In the present study, we focus on the DLPE membrane, which is among the most intensely investigated PE membranes and has also been studied by modeling techniques recently.²⁵

The hydration forces between interacting membrane surfaces have been investigated by many researchers, both experimentally and theoretically.^{1,34,35} Various models have been proposed to explain the observed exponential decay of the repulsion force between approaching membrane surfaces. Nonlocal water polarization in the water layers between the membrane surfaces has been suggested to play an important role in determining the hydration force.^{36,42} In this paper, we attempt to study the water polarization profile in the membrane-water interface and compare the profile obtained to previous theoretical models.

It is well-known that the membrane bilayer interior, or the air phase for a membrane monolayer dispersion, has a positive potential compared to the aqueous solution. This potential, the so-called membrane dipole potential, was first proposed to explain the difference of permeabilities for the hydrophobic ions tetraphenylboron (TPB⁻) anion and tetraphenylphosphonium (TPP⁺) cation,^{47,49} an explanation which has been generally accepted.⁵⁰ The measured dipole potentials are 100–300 mV for membrane bilayers^{51,52} and 300–600 mV for membrane monolayers at the air–water interface.^{48,49} Possible contributions to the dipole potential, as described by McLaughlin⁵³ and Honig,⁵⁴ arise from the membrane head groups, the (glycerol) ester groups, and the oriented water molecules solvating the lipid. Experimental evidence exists for both the ester groups^{55,56} and the solvating water molecules⁵⁷ as possible origins for the dipole potential. Previous modeling studies suggested that the lipid head groups cause a potential in reverse direction to the measured total dipole potential, whereas both the water and the ester groups contribute to the total potential in the right directions.⁵⁸ Another study by Jing and Pullman⁵⁹ on a glyceryl monooleate membrane suggested that the potential arising primarily from lipid dipolar groups can account for the experimentally observed dipole potential and may be important in determining the conformation of gramicidin A imbedded into the membrane. Previous molecular dynamics simulations also suggested dipole potentials of a few hundred millivolts positive inside the membrane bilayer.^{26,60}

The dielectric constant profile of the membrane-water system has been the subject of only a few experimental studies^{61–63} and remains quite unexplained at this point. However, electrostatic potential profile and dielectric constant profile across the membrane are quite important quantities for studying membrane–protein and membrane–drug interactions. One potential application of such profiles is the development of mesoscopic models for the membrane–water interface which could simplify simulations of membrane processes significantly.

In the present study, we have conducted a 200 ps molecular dynamics calculation on a DLPE membrane bilayer patch consisting of 202 lipid molecules and 8108 water molecules. The simulation was conducted under constant temperature (315 K) and constant volume conditions. Long-range Coulombic interactions between all atom pairs were accounted for using the fast multipole algorithm.¹³ Structural properties of the

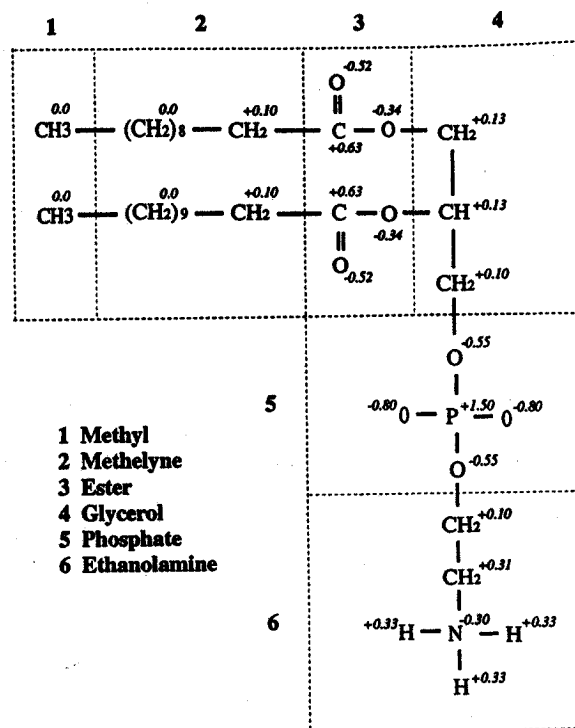


Figure 1. Schematic diagram of the dilauroylphosphatidylethanolamine (DLPE) lipid molecule. Segments of the lipid molecule and the partial charges used in the present study are also shown.

simulated membrane patch were analyzed using the trajectories generated from the last 20 ps of the simulation and suggest that the simulated membrane corresponds to the DLPE membrane in the liquid crystal phase. We calculated the water polarization profile, the electrostatic potential profile, and the susceptibility profile across the DLPE bilayer. Hydrogen-bonding properties of the lipid head group and charge distribution on membrane surfaces were also analyzed. Comparisons were made between the simulated DLPE membrane and a previously simulated POPC membrane bilayer¹² in terms of membrane–water interfacial properties.

Methods

System Simulated. A membrane bilayer consisting of 202 dilauroylphosphatidylethanolamine (DLPE) molecules (Figure 1) was simulated in the present study. The united atom model was used for the DLPE lipid molecules. The partial charges employed for the effective atoms were obtained by modifying the CHARMM parameters and are shown in Figure 1. The CHARMM force field for lipid molecules contains explicit hydrogens. To transfer the corresponding charges to a united atom model, as employed in the present study, we have added the charges of the nonpolar hydrogen atoms to the carbon atoms which they are bonded to and correspondingly changed the atom types for these carbon atoms. For example, the charges of the terminal methyl groups were obtained by adding the charges of the carbon atom and the three associated hydrogen atoms of the CHARMM all-hydrogen model. The charges of the methylene groups were obtained by adding the charges of the carbon atoms and the two associated hydrogen atoms, etc. It turned out that the charges of the methyl and most of the methylene groups were zero, as shown in Figure 1. The charges we use are very similar to the charges used for a previous molecular dynamics study on the DLPE membrane.²⁵ The initial geometry of the DLPE molecules was taken from the crystal structure given in ref 31. One of our objectives to simulate the DLPE membrane is to prepare an equilibrated membrane patch large

enough to study phospholipase A₂-membrane interactions. It is known that phospholipase A₂ interacts with approximately 40 lipid molecules when adsorbed to membrane surfaces.⁶⁴ Hence, we selected 202 lipid molecules, 101 lipids in each monolayer, to form a disk-shaped membrane bilayer with a radius of approximately 41 Å. The membrane simulated in this study would be large enough to study not only the lipid molecules associated with phospholipase A₂ but also the lipid molecules at some distance away from the protein in a phospholipase A₂-membrane complex. The normal of the membrane bilayer was chosen along the *y*-axis, and the center of the bilayer defined the origin of the coordinate system. The DLPE molecule in the liquid crystal phase has a larger surface area (about 50 Å²/lipid) than DLPE in the crystal (about 39 Å²/lipid).³³ Since our simulation method does not allow significant readjustment of the membrane surface area and since the properties of the simulated membrane bilayer depend critically on its surface area as shown by previous simulations,¹² it is very important that the initial structure of the membrane is properly chosen. For the present investigation, we have isotropically scaled the coordinates of the lipid molecules in the *xz*-plane, such that the area per DLPE molecule corresponded to that of the liquid crystal phase. The structure was subsequently energy minimized for 100 steps using the program XPLOR. During the energy minimization, the configurations of the DLPE molecules were optimized and the high internal energy due to the scaling of *x*- and *z*-coordinates was eliminated; the surface area of the constructed membrane bilayer remained unchanged.

Water molecules were then placed on both sides of the membrane. Boxes of water, previously equilibrated with periodic conditions and available from the standard XPLOR package, were added to cover the surfaces of the two membrane sheets. Water molecules were deleted if the oxygen atoms were closer than 1.6 Å to any atom of the lipid bilayer, or if the oxygen atoms were outside of the cylindrical region defined as $\{x^2 + z^2 < 43.0^2 \text{ Å}^2; -40.0 \text{ Å} < y < 40.0 \text{ Å}\}$. A total of 8108 water atoms were selected, which form water layers more than 20 Å thick on both sides of the membrane bilayer. The radius of the water layers in the *xz*-plane was 43 Å, chosen slightly larger than the radius of the lipid membrane to ensure sufficient solvation for lipids in the boundary region.

Our initial structure of the DLPE membrane did not correspond to the membrane in the liquid crystal phase, because the hydrocarbon chains were too ordered and, therefore, the bilayer too thick, nor did it correspond to the crystal phase, due to the larger surface area assigned to the lipid molecules. Also, water molecules were not initially distributed in the membrane-water interface as expected in the multilamellar membrane bilayers. During the course of the molecular dynamics simulation, the effective length of the hydrocarbon chains shrank due to thermal motion, and the chains became disordered. Water molecules penetrated into the membrane head group region, and the thickness of water layers on both sides decreased to approximately 15 Å. Such thickness is the minimum desired for accurate descriptions of the membrane-water interface for the boundary condition employed here (see below). As described in the following section, the position of the two membrane sheets and the boundary conditions for the water molecules were adjusted during the equilibration process until equilibrium was reached.

Experimentally, it is known that the DLPE membrane bilayer hydrates very weakly as compared to PC membranes. In the lamellar structures formed by the DLPE membrane, there are only very thin water layers (5 Å) separating the adjacent

membrane layers.³³ In the present study, the DLPE membrane was solvated by excess water. Furthermore, the membrane patch investigated did not correspond to the membrane lamellar structure³³ since periodic boundary conditions were not employed. Such boundary conditions would have forced us to employ Ewald summation,⁶⁵ which we have not implemented in our programs yet, to account for long-range Coulombic forces properly. We consider it quite unlikely that the excess water placed in the simulated system would cause major effects on the properties of the DLPE membrane. However, future studies are certainly desired to simulate the membrane in a multilamellar environment, through implementation of Ewald summation⁶⁵ in our program, and compare the results to the present study. The recent development of efficient algorithms for Ewald summation for systems with very large elementary cells^{66,67} will allow us to include periodic boundary conditions in future studies.

Simulation Conditions. To maintain the desired shape of the simulated system, in particular, to keep intact the cylindrical shape of the water layers solvating the membrane bilayer (which could change easily due to surface tension), a novel boundary condition was employed in this study. Test calculations were initially conducted using a stochastic harmonic boundary condition, where the atoms in the boundary region were constrained to their starting structure using a harmonic potential, the dynamics of these atoms governed by the Langevin equation.^{68,69} However, such constraints were observed to impose rather rigid structures on the lipid hydrocarbon tails and affect the equilibration of the membrane bilayer, causing an inhomogeneous thickness of the membrane.

We decided then to apply harmonic potentials only to atoms which diffuse outside of a defined region and to omit any constraints for atoms inside the region. Thus, the simulation was carried out in a confined reaction region, defined as a cylinder with a radius of 43.0 Å in the *xz*-plane, with harmonic potential walls. To define the boundary of the cylinder along the *y*-axis, the thickness of the bilayer and the water density profile were calculated. During the equilibration, the overall length of the hydrocarbon tails of the lipid molecules shrank, and, accordingly, the distance between the two monolayers were adjusted subsequently to the experimental data.³³ As a result, the distance between the two bilayers was adapted such that the calculated electron density exhibited two peaks at a distance of 33.0 Å. The water density was calculated in test simulations with different boundary conditions to ensure that the water density remained constant and in agreement with the observed density. The boundaries of the system along the *y*-axis were finally chosen at $y = \pm 35.5 \text{ Å}$.

To constrain the water molecules, the following harmonic potentials were applied to their oxygen atoms:

$$E_{\text{harm}} = \begin{cases} K(y + 35.5)^2 & \text{if } y < -35.5 \text{ Å} \\ K(y - 35.5)^2 & \text{if } y > 35.5 \text{ Å} \\ K(\sqrt{x^2 + z^2} - 43.0)^2 & \text{if } \sqrt{x^2 + z^2} > 43.0 \text{ Å} \end{cases} \quad (1)$$

where $K = 0.5 \text{ kcal}/(\text{mol} \cdot \text{Å}^2)$. A similar, but gentler, potential was applied to all lipid atoms using a force constant $K = 0.2 \text{ kcal}/(\text{mol} \cdot \text{Å}^2)$.

The system was equilibrated for altogether 180 ps at 315 K, a temperature above the gel → liquid crystal phase transition temperature (303.5 K) for DLPE.⁷⁰ During the equilibration, the thickness of the bilayer and the boundary conditions were adjusted as described above. The program MD^{13,71,72} was used for the equilibration. The system was coupled to a heat bath of the desired temperature with a relaxation time of $\tau = 100 \text{ fs}$.

A time step of 1 fs was used for integration of the equation of motion without using the SHAKE algorithm. The electrostatic interactions were calculated between all atom pairs in the system; that is, no cutoff scheme was employed during the equilibration.

After the 180 ps equilibration, the thickness of the membrane bilayer and the water distribution equilibrated as demonstrated by the distribution of various membrane segments and water molecules. A 20 ps simulation (simulation A) was subsequently conducted using the program MD and the same simulation conditions as outlined above. In order to examine the effects of a cutoff of the Coulombic forces, we also conducted simulation B, employing a 8.0 Å shift cutoff using the program XPLOR.⁷³ Simulation B started from the same structure used for simulation A. Simulation B was conducted for 15 ps.

Simulation Programs Employed: MD and XPLOR. The program MD is a library of C functions for a UNIX environment, developed for simulations of biological macromolecules.⁷¹ While many commercial programs are currently available for molecular dynamics calculations, MD was written to give the user easier access to the code and the capability to modify certain functions easily according to the needs of the application.

The energy functions in MD are compatible with the CHARMM⁷⁴ energy functions. However, MD employs new algorithms to calculate long-range Coulombic interactions, namely, the FMA (fast multipole algorithm)⁷⁵ and the multiple time scale algorithm,⁷⁶ and does not use any cutoff scheme. The performance and accuracy of the FMA and multiple time scale algorithms have been documented previously.¹³ For the present study, we employed both the FMA and the multiple time scale algorithm in the calculation for nonbonded forces. The interactions between all atom pairs (including long-range and short-range interactions) were calculated using the FMA library every 20 fs. During intervals of 20 fs, the forces due to long-range interactions (atoms further apart than 7.0 Å from each other) were kept constant and the short-range interactions (atoms within 7.0 Å only) were updated each time step. Simulations in this study were conducted on a Silicon Graphics Crimson workstation with a MIPS R4000 processor. For the 32 808-atom system approximately 3 ps/day dynamics were simulated using the program MD, a performance which is comparable to that of the program XPLOR, with the latter employing an 8 Å cut-off for Coulombic interactions. The program MD and its parallel version PMD, written for parallel computers such as the CM-5 and workstation clusters, are available upon request. (To request a copy of the program MD, please contact Andreas Windemuth at Dept. of Biochemistry, Columbia University, BB-221, 630 W. 168th St., New York, NY 10032, or Klaus Schulten.)

The program XPLOR⁷³ is a widely used molecular modeling program for X-ray and NMR structural refinement. XPLOR implements the CHARMM force field.⁷⁴ Besides using XPLOR for energy minimization and molecular dynamics we employed the program for trajectory analysis, as it uses a very expressive language for data manipulation. In simulation B this program was used for the molecular dynamics calculation. The atom-based shifted cutoff scheme for Coulombic interactions was employed. According to this scheme, the Coulombic force between two charges Q_i and Q_j is⁷³

$$f_{\text{elec}}(R) = Q_i Q_j \frac{C}{\epsilon_0 R^2} \left(1 - \frac{R^2}{R_{\text{off}}^2} \right)^2 \quad (2)$$

where R is the distance between the two charges and $R_{\text{off}} = 8.0$ Å is the chosen cut-off distance. ϵ_0 is the dielectric constant in

vacuum since the dielectric property of the system is represented explicitly by the motion of charged atoms.

Data Analysis. a. Order Parameter. To obtain information on the structure and dynamics in the membrane interior, molecular long-axis order parameters are calculated. Order parameters are related to the average orientation of the methylene group and are defined through the tensor S :

$$S_{ij} = \frac{1}{2} \langle 3 \cos \theta_i \cos \theta_j - \delta_{ij} \rangle \quad (3)$$

where θ_i , $i \in \{x, y, z\}$, is the angle between the i th molecular axis and the membrane bilayer normal. The molecular axes for a methylene group (CH_2) are defined as follows: the x -axis is along the H-H vector, the y -axis is the bisectrix of the H-C-H angle, and the z -axis is defined as the vector perpendicular to the H-C-H plane.²² The deuterium order parameter measured by NMR experiments is given by²³

$$S_{\text{CD}} = \frac{2}{3} S_{xx} + \frac{1}{3} S_{yy} \quad (4)$$

For perfectly extended all-*trans* chains, completely aligned along the bilayer normal, $S_{\text{CD}} = -0.5$. For randomly distributed chains (completely disordered state) $S_{\text{CD}} = 0$. The molecular long-axis order parameter is defined by S_{zz} . In case the molecular motion is isotropic around the z -axis $S_{\text{CD}} = -0.5 S_{zz}$.²¹ The molecular long-axis order parameters were determined in this study from simulation A for all lipid molecules in the simulated membrane and averaged over 50 snapshots at 0.4 ps time intervals.

b. Distribution of Molecular Groups and Angles. To determine the distribution of molecular groups across the bilayer (along the y -axis), and to determine the probability distribution of a few important angles related to the membrane-water interface (such as the angle between the phosphate-ammonium vector and the membrane surface), we only counted the lipid molecules within a given area in the xz -plane. Only lipids whose sn -2 carbon atoms in the glycerol backbone satisfy $x^2 + z^2 \leq 35.0^2 \text{ \AA}^2$ were considered. The following procedure was used to obtain smooth distribution functions despite the relatively few sample points obtained from the simulation. Each statistical realization, e.g., a coordinate or an angle, was considered not as a discrete point but as a Gaussian function:

$$G_i(x) = \frac{1}{\pi^{1/2} \sigma} \exp(-(x - x_i)^2 / \sigma^2) \quad (5)$$

where x is the variable, and x_i is one statistical realization of the variable. The variance σ used in our calculation was 1.5 Å for coordinates and 5° for angles. The distribution probability at x_0 , within a width δx , was then calculated by summing up all the density functions G_i and normalizing according to

$$Q(x_0) \delta x = \left(\sum_i G_i(x_0) / \sum_i 1 \right) \delta x \quad (6)$$

where the summation runs for all the selected atoms (or angles) over many configurations obtained from the simulation.

The density of water molecules was calculated in an analogous way. The averages were carried out for simulation A using different snapshots of the dynamics trajectory. The angle distributions were averaged for the two lipid layers.

c. Water Polarization. The orientational polarization profile along the y -axis was calculated for water molecules whose oxygen atoms satisfy $x^2 + z^2 \leq 35.0^2 \text{ \AA}^2$ to avoid effects from boundary conditions. The polarization profile was calculated

through integration of the charge density:

$$P(y) = \int \rho(y) dy \quad (7)$$

where $\rho(y)$ is the surface charge density of the system in the xz -plane. To calculate the average charge density as a function of y , the system was divided into small slabs with thickness $D = 0.2 \text{ \AA}$ along the y -axis. The charge density was averaged over 150 configurations generated from simulation A. The calculated polarization profile was smoothed using the procedure described in the previous section ($\sigma = 1.5 \text{ \AA}$). The water polarization profile was similarly obtained from simulation B using the configurations of the last 5 ps for comparison.

The contribution to the polarization due to water dipole moments alone was also calculated along the y -axis using

$$P^{\text{dip}}(y) = \gamma(y) p(y) \quad (8)$$

where $\gamma(y)$ is the density of water molecules and $p(y)$ is the average dipole moment of each water molecule at a given y -coordinate. This calculation was carried out for simulation A only.

d. Electrostatic Potential Profile. Several factors contribute to the electrostatic potential profile across the membrane. The experimentally measured dipole potential, which is the potential difference between the membrane interior and the aqueous solution, is the sum of these contributions. We have calculated the charge densities of lipid molecules and water molecules, respectively, along the y -axis. Due to the boundary conditions used in the simulation and due to the difference in the surface area of the lipid and water layer, it is inaccurate to calculate the total potential by integrating over the charge densities, which could be done if periodic boundary conditions had been used.

To calculate the dipole potential, we employed a method consistent with a finite-size system. The average electric field, due to charges of all water as well as all lipid molecules, on a disk with a radius of 35 \AA on the xz -plane, was calculated and integrated while the disk was assumed to be moving along the y -axis. The center of the disk was fixed on the y -axis. Integration of the average electric field on this area gives the average potential profile felt in the central region of the simulated system. Using a smaller radius of 25 \AA for the disk gives a similar potential profile for the membrane-water system studied. The potential profile was calculated for every 0.5 \AA along the y -axis. The calculation was performed on the averaged structure for simulation A (and simulation B) only, since the potential calculation involved numerical integration and was quite time consuming. However, the charge on each atom was treated not as a point charge but rather as a Gaussian charge density, centered around atoms with a variance $\sigma = 1.5 \text{ \AA}$. The potentials due to water and lipid molecules were determined separately, and the total potential was calculated by adding the two contributions.

e. Susceptibility Profile. Susceptibilities of model systems were determined previously, using linear response theory,⁷⁷⁻⁷⁹ for homogeneous systems like water^{80,81} employing the formula

$$\chi = \frac{4\pi \langle M^2 \rangle}{3VT} \quad (9)$$

where M is the total dipole moment of the system, V is the volume of the system, and T is the temperature at which a simulation is conducted. We modified this method in the present study to obtain a susceptibility profile for the simulated membrane system along the y -axis. To calculate the suscepti-

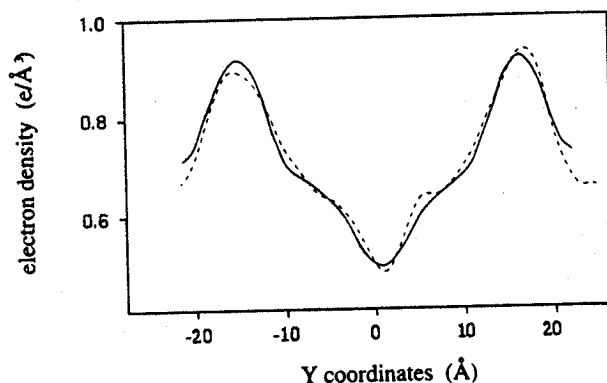


Figure 2. Electron density profile of the simulated DLPE membrane-water system (dashed line) and the electron density profiles observed for the DLPE membrane in the liquid crystal phase for the DLPE membrane (solid line, data taken from ref 33, in arbitrary units).

bility profile, the system was sliced into 1.0 \AA thick slabs along the y -axis. The susceptibility of each slab was calculated using the fluctuation of the polarization in that particular slab according to

$$\chi(y) = \frac{4\pi \langle (M_y(y) - \overline{M_y(y)})^2 \rangle}{AdT} \quad (10)$$

where $M_y(y)$ is the polarization along the y -axis due to all charges located in the slab, A is the area of the slab in the xz -plane, and d is the thickness of the slab (1.0 \AA). $\overline{M_y(y)}$, the average polarization along the y -axis due to all charges in the slab, was subtracted to obtain the fluctuations of the polarization. This quantity was omitted in previous studies for homogeneous systems, where it should be zero,^{80,81} but could not be omitted for the membrane-water interface because the system is inhomogeneous and there exist permanent dipole moments along the y -axis which lead to the membrane dipole potential. Our method to calculate the dielectric constant is very similar to that used by Warshel *et al.* for protein-water systems,⁸² except that these authors applied the method to spherical regions while we applied it to cylindrical disks.

To obtain the susceptibility profile of the system, fluctuations of the polarization were calculated using the 20 ps dynamics trajectory from simulation A. Only the water molecules, whose oxygen atoms satisfy $x^2 + z^2 \leq 35.0^2 \text{ \AA}^2$, and the lipid molecules, whose $sn-2$ carbon atoms in the glycerol backbone satisfy the same condition, were considered. Thus, the susceptibility was calculated for a cylindrical region with the area in the xz -plane of $A = 35^2\pi \text{ \AA}^2$.

Structural Properties of the Membrane

Electron Density and Order Parameter. The shape of the electron density profile, averaged over simulation A, is compared in Figure 2 with the profile observed for a DLPE membrane in the liquid crystal phase. The center of the lipid bilayer shows a characteristic minimum of the electron density.

The molecular long-axis order parameters for the $sn-1$ and $sn-2$ chains of simulation A are compared in Figure 3 with the order parameters experimentally measured for the DPPC membrane at $51 \text{ }^\circ\text{C}$. The carbon atom next to the carbonyl group of each hydrocarbon chain is denoted as carbon atom 2 in this study, and the terminal methyl group is denoted as carbon atom 12 (their molecular long-axis order parameter cannot be calculated). The simulation for the DLPE membrane was carried out at $11.5 \text{ }^\circ\text{C}$ above its phase transition temperature,

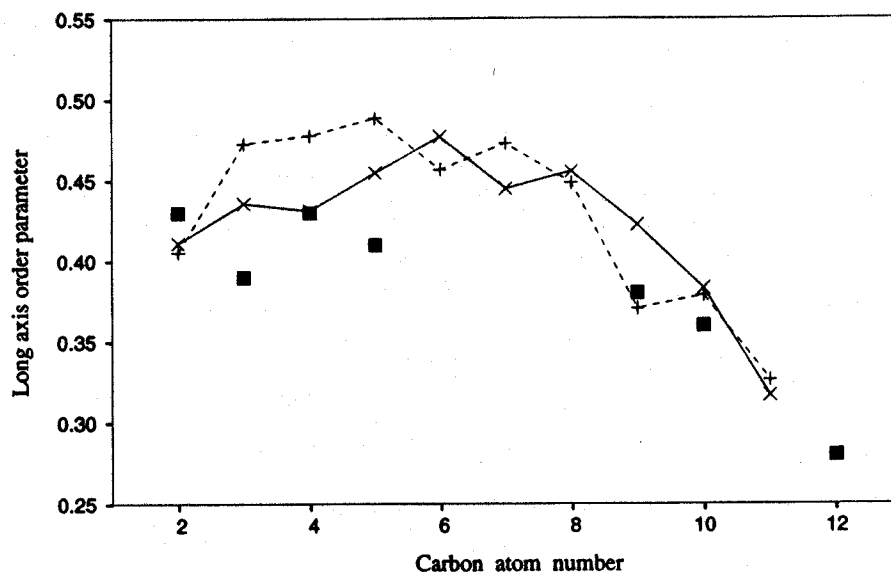


Figure 3. Molecular long-axis order parameters calculated for the simulated DLPE membrane as compared to the experimentally measured order parameter for the DPPC membrane: (x) order parameters for the *sn*-1 chain of the simulated DLPE membrane; (+) order parameters for the *sn*-2 chain; (■) measured order parameter for the DPPC membrane⁸³ at 51 °C.

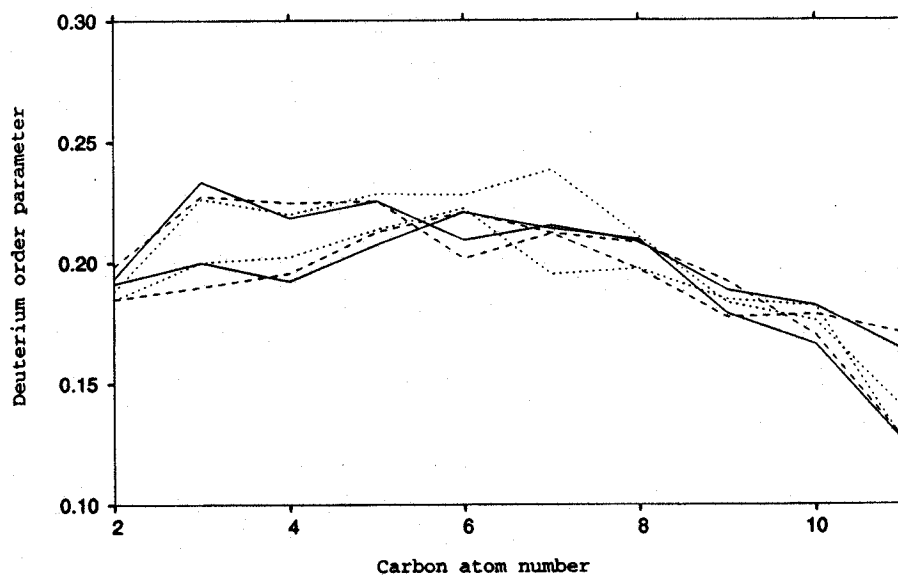


Figure 4. Deuterium order parameter of the membrane bilayer of the *sn*-1 and *sn*-2 chains obtained from the structures at 0.2 ps (solid line), 10.2 ps (dashed line), and 18.2 ps (dotted line) of the final 20 ps of our 200 ps simulation.

whereas the experimental order parameters for the DPPC membrane were measured at 10 °C above its phase transition temperature.⁸³ Because DLPE lipid molecules have quite short hydrocarbon tails, and because of the difference in the head group of the PE and PC membranes, a direct comparison is not possible. However, the calculated order parameters show the characteristic plateau up to carbon atom 8 and a decrease in the order parameter along the tails of the hydrophobic chains. The order parameters calculated for carbon atoms 3–8 are slightly higher than the order parameter for DPPC, as given by deuterium NMR studies.⁸³ Our simulation does not reproduce the characteristic dip in the order parameter for the carbon atom at position 3 very well, which is probably due to a short simulation time or due to the united atom model employed which does not describe very accurately the packing between lipid hydrocarbon chains. Such a difference between the simulated and the experimentally observed order parameter profiles was also noticed in our previous study on the POPC membrane¹² as well as in other simulation studies.²⁵

We only present the average structural properties for the membrane during the last 20 ps simulation time here. The

electron density and the order parameter of the two chains are stabilized during the last 20 ps, suggesting that a 180 ps equilibration is long enough for the present analysis. The deuterium order parameters of the membrane bilayer at 0.2, 10.2, and 18.2 ps of the last 20 ps simulation are shown in Figure 4; no significant differences in the order parameter profiles can be observed for the three snapshots, except for that caused by the fluctuation of the system. However, since the characteristic time scale for lipid motion is nanosecond or longer for lipid diffusion, the structure of the membrane bilayer cannot be thoroughly equilibrated during simulation times which are accessible using our current computational resources.

Lipid Group Distribution and Water Density. The distribution of various segments of the lipid, as defined in Figure 1, and of the water molecules is presented in Figure 5. The head groups of the lipid molecules are seen to be distributed over a width of about 15 Å. The width is somewhat larger for the lower lipid layer ($y < 0$) compared to the upper layer ($y > 0$), the difference being due to a statistical error arising from the relatively small sample size. The water molecules are seen to penetrate up to the ester groups of the hydrocarbon tails;

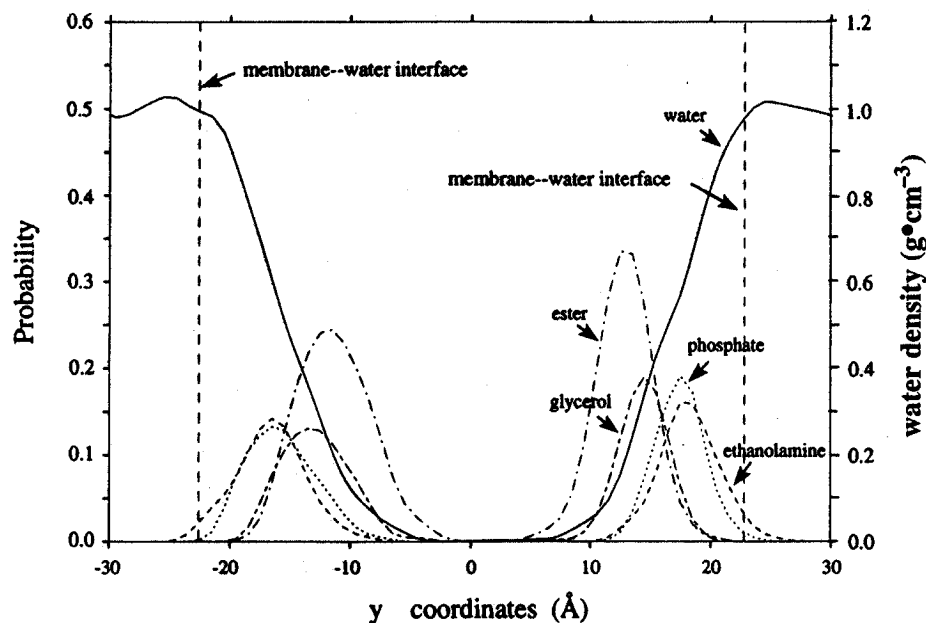


Figure 5. Distribution probabilities of the lipid segments as specified in Figure 1 and water density across the membrane: left scale, distribution probabilities of the lipid segments; right scale, water density ($\text{g}\cdot\text{cm}^{-3}$).

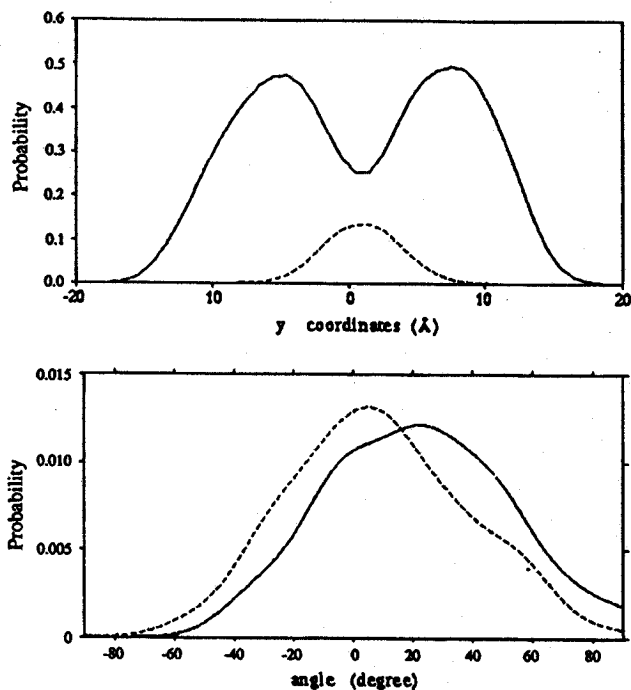


Figure 6. Top: distribution probabilities of the methylene (solid line) and the methyl (dashed line) groups across the simulated DLPE membrane. Bottom: distribution probabilities of the angle between the phosphate-ammonium vector (solid line) and the carbonyl groups (dashed line) and the membrane surface.

this penetration depth has also been suggested by experimental studies⁸⁴ and previous simulations. We determined the approximate number of bound water molecules per lipid molecule by counting the waters within the range of the two dashed vertical lines in Figure 5. The spacing between the two lines is 46.1 Å and corresponds to the spacing between DLPE lamellar membranes.³³ Roughly 10.6 waters per lipid are found in this range; this compares well with 9–10 waters suggested by experimental studies to be bound per lipid head group.^{33,85}

Figure 6 (top) shows the distribution of the methylene and the methyl groups of the DLPE bilayer. The terminal methyl group is observed to distribute over a width of about 20 Å in the center of the membrane bilayer. Even though the distribu-

tion of the methyl groups is broad, they do not distribute over the entire range of the membrane, as do the methylene groups. Such distribution for terminal methyl groups of lipid hydrocarbon tails in the membrane bilayer has also been observed for the DOPC membrane.⁸⁴ Figure 6 (bottom) displays the distribution of the angle between the phosphate to ammonium vector (PN vector) and the membrane surface, as well as the angle between carbonyl groups and the membrane surface. An average tilt of +20° toward the aqueous solution is found for the PN vector. An angle of about +8° is found between the ester carbonyl groups and the membrane surface, with the carbonyl groups tilting toward the membrane-water interface. A small tilt of the carbonyl toward the aqueous phase has been suggested previously and might contribute to the membrane dipole potential^{55,56} analyzed in the following sections.

Interfacial Properties of the Membrane

Water Polarization. The total water polarization (solid line) and the polarization due to dipole contribution only (dashed line) are shown in Figure 7. The total water polarization is also obtained for the trajectory from simulation B (by integrating the charge density) and is shown as a dotted line in Figure 7. The polarization of water shows two peaks in regions where the membrane head groups are located. The charge density of the water molecules in the head group–water interface almost exactly cancels out the charge density due to lipid head groups located in this region (not shown). Therefore, the water molecules behave as a high-dielectric-constant medium, and their polarization profile reflects the lipid head group distribution. Very small polarization arises for water molecules located in the regions where no lipid head groups are found, *i.e.*, at $y < -25.0$ Å or $y > 25.0$ Å. The two small peaks in the polarization profile close to the system boundary are probably induced by the water–vacuum interface. According to experiments,⁸⁶ water molecules would orient themselves with the hydrogen atoms pointing toward the water–hydrophobic interface such that the hydrophobic region would have a positive electrostatic potential relative to the aqueous solution. Such behavior is qualitatively in agreement with the water polarization profile obtained for waters at the system boundary shown here and is probably not related to the membrane–water interface and, thus, not of importance for our study.

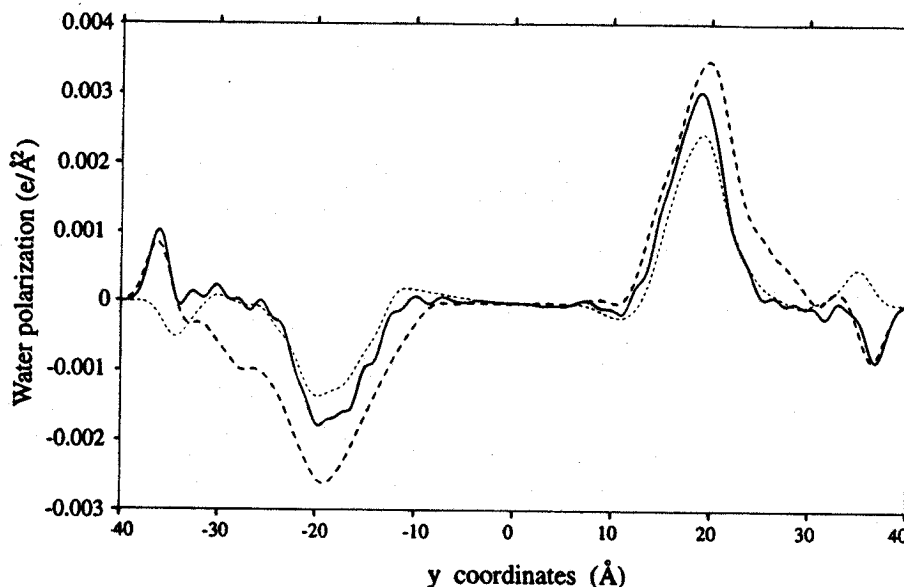


Figure 7. Water polarization profiles of the simulated DLPE membrane system along the y -axis (solid line) total water polarization obtained from simulation A (with no cut-off); (dotted line) water polarization due only to dipole contributions from simulation A; (dashed line) total water polarization obtained from simulation B (with 8 Å cutoff).

A shifted cutoff scheme for the Coulombic interaction, as adopted in simulation B, causes profound differences in the water polarization. The most prominent effect is a wider polarization profile, which indicates more water layers are affected by the membrane head groups as compared to that of simulation A. Such an effect is most likely due to the water molecules some distance away from the membrane surface which would interact with only some of the charged membrane head groups because of the cutoff scheme. For example, the water molecules might interact with the ethanolamine group, which is within 8.0 Å in distance, but would not interact with the phosphate group farther away. The net result is an artificial long-range potential which would not be present if all the atom pairs were included in the calculation of electrostatic forces using the fast multiple algorithm, even though the cutoff scheme itself includes only short-range Coulombic interactions compared to the fast multipole algorithm.

We have also calculated, for comparison, the water polarization for a POPC membrane, using molecular dynamics trajectories reported in ref. 12. The magnitude of the polarization for the POPC membrane-water interface, presented in Figure 7, is about twice as large as for the DLPE-membrane interface. The width and shape of the water polarization profile of the POPC membrane are similar to that of the DLPE membrane (Figure 8).

Membrane Dipole Potential. The calculation of the electrostatic potential of the system has been described in the Methods section. Figure 9 (top) shows the potential profile due to the water molecules and due to the lipid molecules. There is a significant decrease (negative inside) of the potential due to the lipid phosphate-ammonium dipoles when moving across the lipid head group-water interface into the membrane interior. A smaller potential increase (positive inside) occurs in the region where the ester groups are located, due to the partial charges of the carbonyl groups. Not surprisingly, the potential due to the water molecules almost completely cancels the potential due to lipid head groups in the interfacial region, and the cancellation is not as complete in the region where the ester groups are located, i.e., where the water density is much lower.

The resulting total electrostatic potential is shown in Figure 9 (middle). The potential difference between membrane interior and the aqueous solution, or the membrane dipole potential,

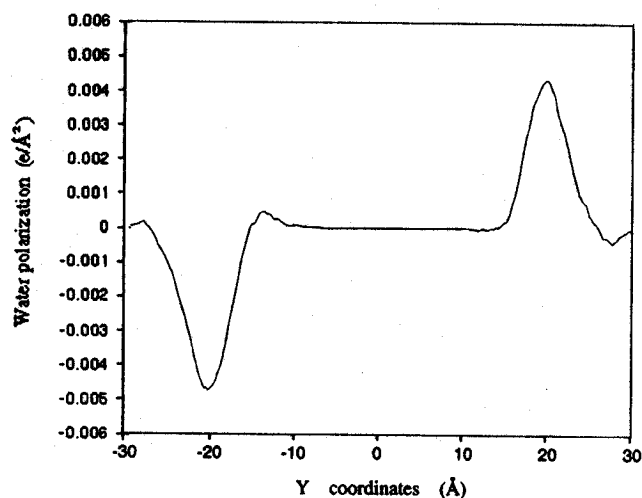


Figure 8. Water polarization profiles of the previously simulated POPC membrane system along the y -axis.

determined from our simulation, is 600 mV. The dipole potential measured for the DLPE monolayer (air-water interface) is 450 mV.^{51,52} The dipole potential measured for membrane bilayers is usually smaller than that of the monolayers formed between air-water interfaces, typically 100–150 mV less.^{49,87} The reason for this difference is not well understood; McIntosh *et al.*³⁷ suggested that the dipole potential measurements with bilayers depend on large probes that perturb the interface. The calculated potential profile suggests that the main contribution to the dipole potential comes from the ester groups (450 mV), and the overcompensation of the contribution due to oriented water in the head group-water interface, i.e., the contribution from hydration, is about 150 mV. Our model does not use explicit hydrogen atoms for the hydrocarbon tail and does not include the effects due to atomic polarization, and their effects on the dipole potential are neglected in the simulation. A higher dielectric constant than assumed in the ester group regions would also cause a smaller dipole potential across the membrane. Using an all-hydrogen model or employing a more realistic dielectric constant in the simulation might improve the agreement between the simulated dipole potential and the experimental results.

The membrane dipole potential has also been calculated for

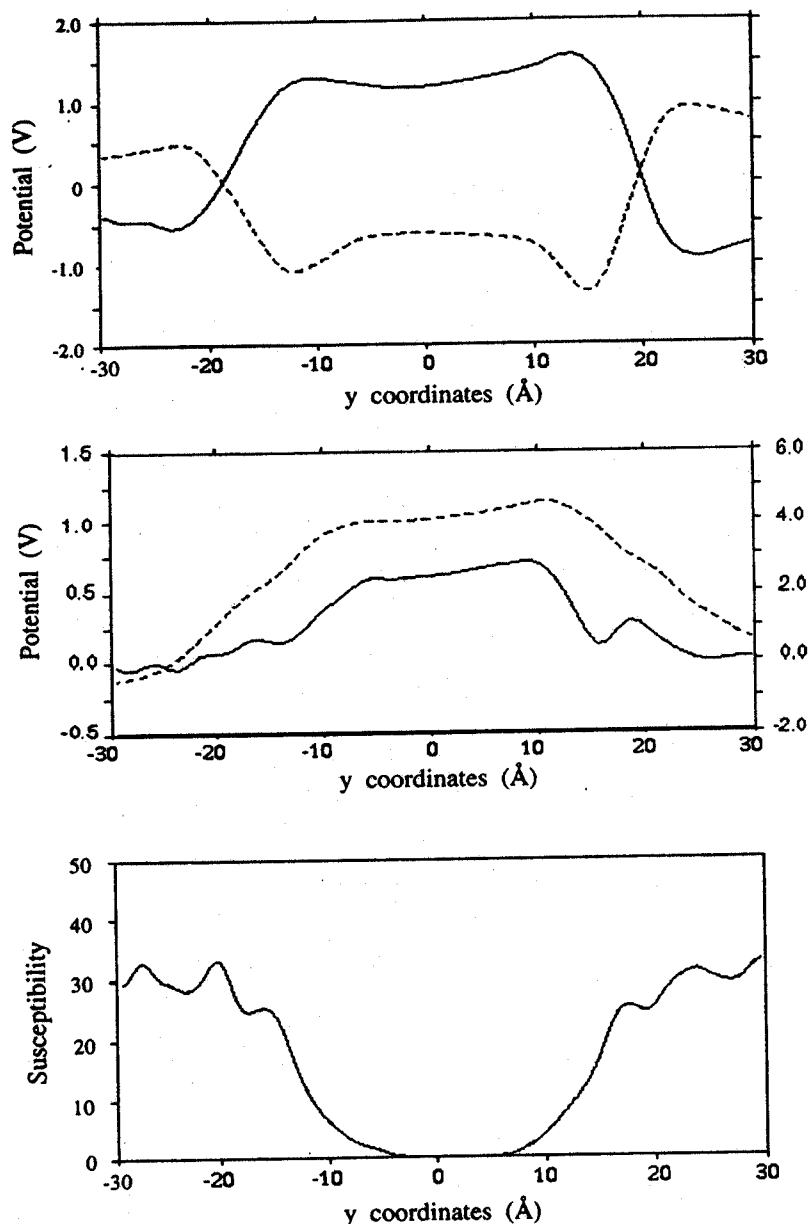


Figure 9. Top: electrostatic potential profiles across the membrane due solely to contributions from water molecules (solid line) and lipid molecules (dashed line). Middle: the total potential profile across the membrane; solid line, simulation A (left scale); dashed line, simulation B (right scale). Bottom: the susceptibility profile across the membrane, calculated using the trajectory obtained in simulation A.

the average structure generated from simulation B. The same method as in the case of simulation A is used for the evaluation of the potential. The resulting potential profile is shown in Figure 9 (middle). The potential is about seven times larger in magnitude compared to the potential predicted by a simulation without cutoff, mainly due to a significant overestimate of the potential due to oriented water molecules. It appears that the error in the water polarization profile leads to the large overestimate of the membrane potential: this implies that the conformation equilibrated in a simulation with cutoff cannot be used to determine the potential profile.

Susceptibility. The susceptibility of the system is calculated along the y -axis as described in the Methods section. The susceptibility of the lipid head group–water interface, as shown in Figure 9 (bottom), is found to be approximately 30. The susceptibility profile decreases slowly in the head group–water interface and decreases rapidly in the region in which the ester groups are located. The calculated susceptibility profile is in reasonable agreement with previous measurements of membrane bilayers^{61–63} which suggested a dielectric constant of 30 for the hydrophilic head groups and a dielectric constant of 6–10

for the ester groups. The susceptibilities for the water layers outside the membrane surface are 30–40 in our simulation, which is much less than the expected value for bulk water (~ 78). There are a few possible reasons for this disagreement. First, the dielectric property for the water molecules close to the membrane surface might be different from bulk water. In our simulation, only a few layers of neat water are included (the thickness of the water layer is only 15 Å), and their behavior might be somewhat between bound water and bulk water. Therefore, the dielectric constant could also be lower. It has been reported by Warshel *et al.* that boundary conditions and cutoff play a major role in determining the dielectric constant for a finite system.⁸² Inclusion of the reaction field was shown to be essential in obtaining realistic dielectric constants for simulated water droplets. Periodic boundary conditions and Ewald summation of Coulombic forces might provide more realistic dielectric properties. Previous studies have shown that the water models currently used in simulations might have a lower dielectric constant than real water. Dielectric constants of 34.0 and 53.0 were found for the MCY and the TIP4P water models at 293 K.^{80,81} Berendsen *et al.* suggested that polariza-

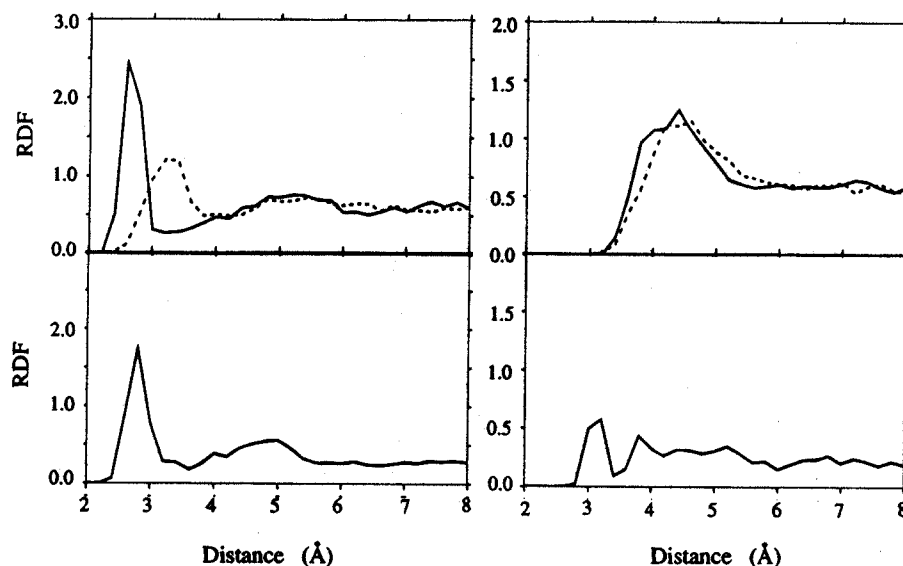


Figure 10. Radial distribution functions (RDFs) around the lipid head group obtained from the present simulation of DLPE and the previous simulation of POPC membranes.¹² Left top: RDFs of water oxygen (solid line) and water hydrogen atoms (dashed line) around the ammonium nitrogen atoms of the DLPE membrane. Left bottom: RDF of lipid oxygen atoms around the ammonium nitrogen atoms of the DLPE membrane. Right top: RDFs of water oxygen (solid line) and water hydrogen atoms (dashed line) around the choline nitrogen atoms of the POPC membrane. Right bottom: RDF of lipid oxygen atoms around the choline nitrogen atoms of the POPC membrane.

tion effects might be important to obtain a more realistic description of water.²³ However, simulations using polarizable water models did not show much improvement in obtaining a more realistic dielectric constant.⁸⁸

Interlipid Hydrogen Bonding and Membrane Surface Charge Distribution. Figure 10 shows the radial distribution function (RDF) of oxygen atoms of water molecules as well as of lipid phosphate groups around the ammonium nitrogen atom of DLPE. The RDFs are normalized by the density of oxygen (or hydrogen) atoms in bulk water and, therefore, do not necessarily approach 1.0 at large distances.

Counting only the number of oxygen atoms in the first coordination shell (within a distance of 3.2 Å), there are on average 3.4 water oxygen atoms and 2.5 lipid oxygen atoms around one ammonium group. Similarly, we found 10.5 water hydrogen atoms and 3.0 lipid ammonium hydrogen atoms around each phosphate group of the DLPE membrane in the first hydration shell (within 4.0 Å). The head groups of the DLPE membrane form interlipid hydrogen bonding to a certain extent, but more hydrogen bonds are formed with water molecules, particularly for the bulky phosphate group. The interlipid hydrogen bonding of the DLPE membrane in the liquid crystal phase appears to be weaker when compared to the hydrogen-bonding network formed in the crystal structure.³¹

We determined also the RDFs for the POPC membrane, exploiting the trajectories reported in ref 12. The result is compared in Figure 10 with the RDFs of the DLPE membrane. In the PC membrane, the N—CH₃—O(water) RDF peaks at 4.4 Å, and there is no preferential orientation of water around the choline head group. In the PE membrane, the peak of the N—H—O(water) RDF is at 2.8 Å, and there is significant hydrogen bonding between the ammonium group and waters in the first hydration shell. These results support the suggestion that PC membranes induce formation of clathrates in the nearby waters.^{89,97} We also find that there is, on average, only one lipid oxygen atom in the first hydration shell of the choline group in POPC, which indicates that the interlipid electrostatic interaction in PC membranes is weaker than in PE membranes.

The charge density of the DLPE membrane surface is calculated using the averaged structure from simulation A. Because the charges of the lipid molecules are distributed in

the three-dimensional space, there is not a well-defined two-dimensional surface on which the charge density could be calculated: such a surface is only defined for the purpose of the analysis. In this study, we have calculated the surface charge density by projecting the 3-D charge density of the lipid molecules into the *xz*-plane. Each charge atom is treated as a Gaussian function with $\sigma = 1.5$ Å, as described previously. The calculation was performed for 10 000 cells in the area defined by $\{-25.0 \text{ Å} < x < 25.0 \text{ Å}; -25.0 \text{ Å} < z < 25.0 \text{ Å}\}$, and the size for each cell is 0.5 Å along the *x*- and *z*-axis. The calculated charge density is shown in Figure 11. The charge distribution and, as a consequence, the electrostatic field, on the membrane surface is clearly inhomogeneous. We have calculated the radial correlation function $g(r)$ of the surface charge density defined by

$$g(r) = \langle \rho(\vec{r}_0) \rho(\vec{r}_0 + r\vec{t}) \rangle / \langle \rho(\vec{r}_0)^2 \rangle \quad (11)$$

where \vec{r}_0 is a vector in the *xz*-plane which defines the position of any cell and \vec{t} is a unit length vector in the *xz*-plane with arbitrary direction. Ensemble average is performed over \vec{r}_0 and \vec{t} by calculating the correlation using all cells in the area $\{-25.0 \text{ Å} < x < 25.0 \text{ Å}; -25.0 \text{ Å} < z < 25.0 \text{ Å}\}$. The correlation functions $g(r)$, calculated up to a distance of 40 Å separately for the two membrane monolayers, are shown in Figure 12. To compare the distribution of surface charge densities of PE and PC membranes, we also calculated the correlation functions $g(r)$ for a POPC membrane bilayer using the coordinates from the simulation reported in ref 12 (see Figure 12). For both the DLPE and the POPC membrane, long-range correlations in surface charge density are found. However, in both cases the correlation length is estimated to be within 8–10 Å, and the behavior of the correlation functions in DLPE and POPC membranes is very similar.

Discussion

In order to model biological membranes at the atomic level, in particular for studies of protein—membrane and drug—membrane interactions, we had previously constructed and simulated a POPC membrane bilayer¹² of large size. To test the accuracy of the model, deuterium order parameters, spatial

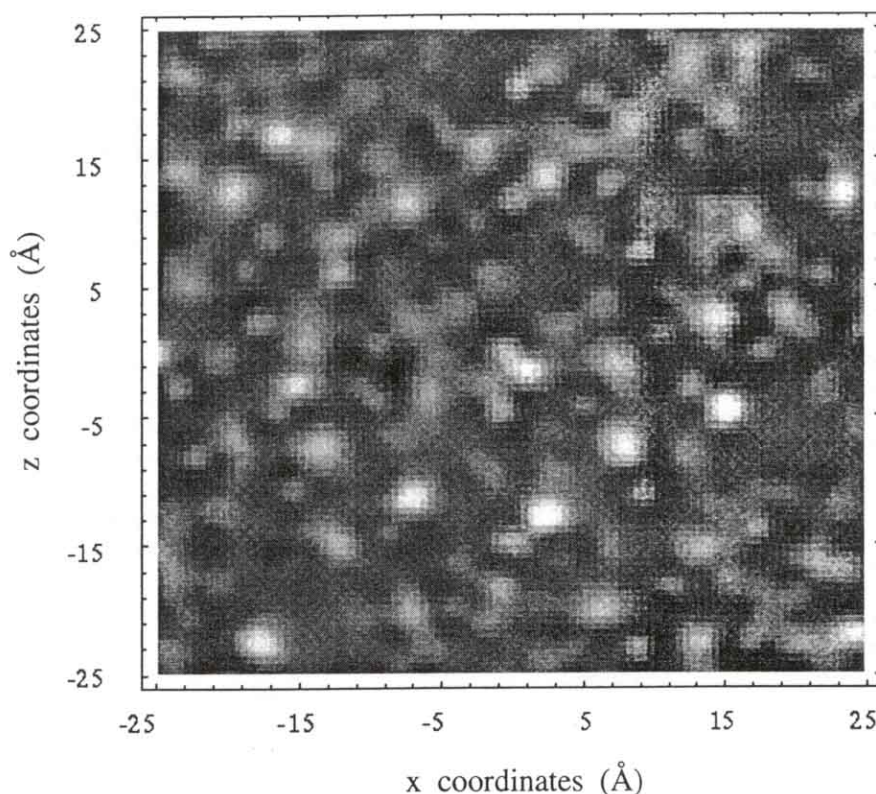


Figure 11. Surface charge densities obtained for one monolayer of the simulated DLPE membrane bilayer. Bright regions correspond to positive charge densities, and dark regions correspond to negative charge densities.

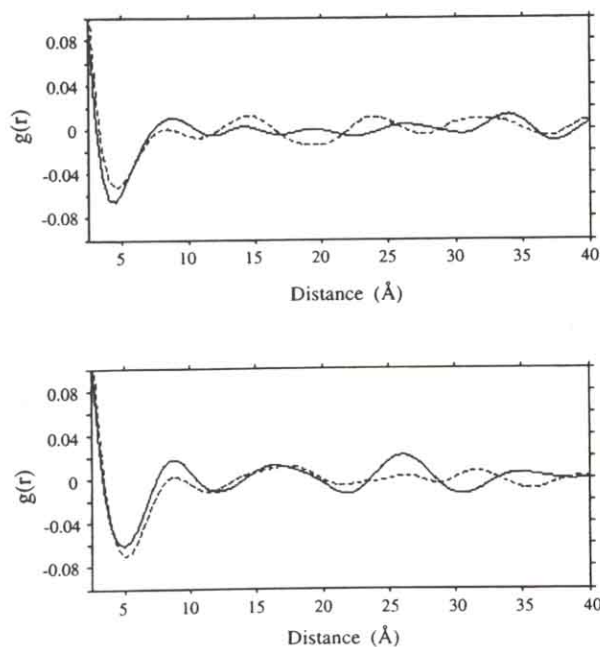


Figure 12. Radial correlation functions $g(r)$ of the surface charge density calculated for the DLPE membrane (upper) and the POPC membrane (lower). The correlation functions were calculated separately for the two monolayers in each membrane and are shown as a solid line and a dashed line, respectively.

distribution of lipid segments and of water, the head group angles relative to the membrane normal, the lateral diffusion constant were calculated and compared with observations. The results suggested that the membrane model used was in reasonable agreement with actual membranes.

In this study, a patch of a DLPE membrane bilayer with a diameter of more than 80 Å (with 101 lipid molecules in each monolayer), with a 15 Å water layer on each side of the

membrane, was constructed and simulated. All atoms, except the hydrogen atoms attached to nonpolar carbon atoms, were described explicitly. The simulated system involved 32 808 atoms. The study of the DLPE membrane was motivated by the specific role which the PE membrane plays in many protein-membrane complexes, such as in the case of the protein phospholipase A_2 .^{90,91} The membrane patch simulated here is large enough to be used in further studies of phospholipase A_2 -membrane complexes. The width of two lipid layers was adjusted during the simulation to agree with experimentally measured electron density profiles. To avoid possible artifacts in the description of the membrane-water interface, long-range Coulombic interactions were calculated explicitly; that is no cut-off scheme was used.

General Properties. A 200 ps simulation had been carried out for the present study, which required more than 2 months of calculation on a Silicon Graphics workstation with a MIPS R4000 processor. Such short simulation time is not sufficient to study many properties of the membrane bilayer. Electron density profile, molecular long-axis order parameters, distribution of lipid segment and water penetration, and the average angle of the lipid head group to membrane surface were calculated in this study. The results indicate that the simulated membrane corresponds to a membrane bilayer in the liquid crystal phase. The order parameters of the simulated membrane are a little higher than the order parameter measured for a DPPC membrane at comparable temperatures. The distribution of membrane segments and water molecules does resemble the observed properties of DOPC membrane bilayers.

A particular emphasis in this study was placed on analyzing properties of the membrane-water interface, i.e., the water polarization, the dipole potential profile, and the susceptibility profile along the membrane normal. We have also analyzed, as a complement to a previous study,¹² other properties of the lipid, such as the hydrogen-bonding properties of the lipid head

group and the membrane surface charge distribution. Such properties are very important in studying protein–membrane and protein–drug interactions and may serve to construct simpler mesoscopic models of membranes. One promising feature of the present approach is that it allows one to obtain the free energy profile for drug molecules diffusing through the membrane bilayer, by calculating contributions from electrostatic interactions, hydrophobic interactions, and steric interactions to lipid hydrocarbon tails.

Theoretical Models for the Hydration Force. An early model for membrane hydration forces was proposed by Marčelja and Radic based on a Landau-type expansion of the free energy density.³⁶ The change in the free energy, caused by the partial orientation of the interbilayer water between two membrane surfaces separated by a distance d_w , is described by the free energy terms associated with the water polarization, by its spatial variation, and by the coupling between the water polarization and external orienting polarization field. The model suggested that the hydration force decays exponentially as d_w is increased. The decay length of the hydration force λ , observed to be close to 2.0 Å, was suggested to be the correlation length of the water polarization and, therefore, is a property of water itself. The magnitude of the hydration force is determined by the water polarization at the membrane surface. Later studies by Simon and McIntosh³⁷ suggested that this magnitude can be further related to the membrane dipole potential, assuming that the dipole potential provides the electrostatic field that orients the solvating water molecules at the membrane–water interface. The authors tested through experiments the relationship between the hydration force and the dipole potential as suggested in their model.

The Marčelja–Radic model assumed an infinitely thin membrane surface and suggests a nonlocal behavior of water polarization at the membrane–water interface.^{38,39} Such assumptions are, however, questionable. Experiments with different surfactant and lipid bilayers in water have yielded values for λ varying from 1.0 to 3.0 Å.³⁴ With such a large variation, λ does not correlate necessarily to the size of a water molecule. Simulation studies on a mica surface and on a lecithin surface did not reveal the proposed exponential decay of water polarization,⁴⁰ and the membrane–water interface has a significant thickness. Another simulation study on a DLPE membrane in the gel phase suggested the hydrogen-bonding profile as the order parameter instead of the water polarization.⁴¹ Cevc⁴² attempted to incorporate the thickness of the membrane–water interface into the original model and suggested for relatively thick membrane interfaces that the hydration forces might be stronger than predicted by the Marčelja–Radic model and would decay on the length scale of the interfacial thickness rather than λ . In a recent simulation study,²⁶ it was suggested that the water polarization on the surface of a liquid crystal phase membrane is mainly determined by the distribution of membrane head groups. Another model, proposed by Israelachvili and Wennerström,^{43,44} went further to suggest that the so-called “hydration” forces are not due to water structures but rather originate from entropic repulsion of the lipid molecules that protrude from the fluid-like membrane surfaces through thermal motion. Genuine hydration is suggested to play only an indirect role through determining the hydrated sizes of the protruding groups. Our previous studies on POPC membrane bilayers¹² support this view to some extent.

An alternative view of the origin of the hydration force has been suggested by Kornyshev and Leikin⁴⁵ and Rand *et al.*⁴⁶ In their model, inhomogeneous membrane surfaces are considered; that is, the (dipolar) charge density on membrane surfaces is assumed to be fluctuating with a certain correlation length.

According to this model, the decay length of the hydration force is determined not only by the decay length of water polarization but also by the nature of the interface. When the correlation length of the membrane surface charge density is smaller than the decay length of water polarization, the hydration force is suggested to depend mainly on the property of the membrane surface, and Kornyshev and Leikin argued that this is indeed the case for biological membranes. This model was applied to explain the observed weaker hydration for PE membranes since PE membranes were suggested to have stronger correlation in surface charge density due to interlipid hydrogen bonding.⁴⁵

Polarization of Water Molecules. Along with a recent molecular dynamics study of other membranes,²⁶ the calculated water polarization and lipid head group distribution in this study suggest that the polarization due to water molecules almost completely cancels the polarization due to lipid head groups. The solvating water molecules in the membrane–water interface, thus, behave like a classic medium of high dielectric constant, and nonlocal effects due to intrinsic water correlation length are hardly observed. It appears that the decay length of the distribution of lipid head groups in the membrane–water interface (which is about 2.0 Å obtained by a monoexponential fit for the two membrane sheets simulated in the present study) plays an essential role in determining the decay length of the water polarization in the interfacial region.

The role of water in screening charge–charge interactions in proteins has been previously demonstrated by Warshel and Russel^{92,93} and has been demonstrated here for screening of charged membrane surfaces. The water polarization profile calculated in this study had been averaged over the xz -plane, and the conclusions we draw on the behavior of the solvating water molecules are valid only on an average.

Due to the fact that periodic boundary conditions were not employed in our simulation, our system does not correspond to a membrane system with lamellar structure, to which we compare our results, e.g., the distribution of lipid segments and water. A simulation of lamellar membranes employing corresponding periodic boundary conditions, Ewald summation of Coulombic forces, and water layers which correspond to the small degree of hydration of lamellar membrane systems is highly desirable.

These limitations of the simulation prohibit an accurate description of the properties of bulk water some distance away from the membrane surface and also prevents the decay length of water polarization from being accurately determined.

Membrane Dipole Potential. The calculated electrostatic potential across the membrane can be compared to the measured dipole potential for DLPE monolayers.^{51,52} Our study suggests that the main contribution to the dipole potential arises from the ester groups, namely, 450 mV for the total potential increase, whereas the hydration of the lipid head group contributes only 150 mV. This result is in agreement with other modeling studies.^{58,59} Two recent experiments support our results on the membrane dipole potential: a study on the membrane monolayers at the argon–water interface⁹⁴ has shown a linear relationship between the measured dipole potential and the surface concentration of the membrane dipoles; the authors in ref 94 also suggested a nondipole contribution arising from the oriented water molecules which can be larger than 100 mV, in line with the value we report here; a second study⁹⁵ compared the dipole potential in both DPPC/cholesterol and DPPC/6-ketocholestanol membranes and suggested that introducing further carbonyl groups in the latter membrane caused the observed increase in dipole potential compared to the DPPC/

cholesterol membrane. Recent experiments by Gawrisch *et al.*, however, contradicted our findings in that they suggest a contribution from the membrane ester group of only about 110 mV for DPPC and DHPC membranes.⁵⁷

The measured dipole potentials of lipid membrane monolayers are usually larger than measured for bilayers by 100–150 mV. The dipole potential obtained in our study compares better with the potential measured for the air–water monolayer. We notice that this is true also for a number of other molecular dynamics studies.^{26,60} The reason for such a difference is not clear. McIntosh *et al.*³⁷ suggested that the dipole potential measurements with bilayers depend on large probes that perturb the interface,³⁷ and the dipole potential measured for the monolayer might be a more accurate description of unperturbed biological membranes. If this is indeed true, then the dipole potential obtained from molecular dynamics simulations should agree better with the observed data from the membrane monolayer rather than from the membrane bilayer.

The dipole potential obtained from simulation depends very much on the partial charges assigned to the lipid molecules and on the dielectric property of the simulated system. It is also possible that the calculated dipole potential is larger than the measured dipole potential for a membrane bilayer due to errors arising from the force field employed. The methylene groups and the methyl groups are not charged in our force field, and we did not consider atomic polarization effects in our simulation. The dielectric constant of the hydrocarbon region resulting from such a force field is effectively 1, whereas in reality it is probably 2 or larger. An underestimate of the dielectric constant would in turn cause an overestimate of the dipole potential. However, in view of the limitation of the MD simulation technique, we regard our agreement with observation as very satisfactory.

To understand better the origin of the membrane dipole potential, simulation studies on other membranes, such as the DPPC membrane, and heterogeneous membrane systems, such as the DPPC/cholesterol membranes, would be desired. Comparison of the simulated results with the observed dipole potential of these systems would provide more information on the accuracy of the molecular dynamics technique as well as on the contributions of various factors to the total dipole potential.

Simon and McIntosh³⁷ suggest that the water polarization in the membrane–water interface and the dipole potential are related. Our results suggest, however, that the membrane ester groups are the origin of the dipole potential, while the water polarization nearly cancels the contribution of the charges of the phosphatidylethanolamine head groups to the dipole potential. This suggestion is corroborated by the observation that the water polarization of the POPC membrane is twice as large as that of the DLPE membrane, due to the difference of the head group in the two membranes. However, the dipole potentials measured for PC and PE membrane monolayers are not too different. However, other experiments⁵⁷ support the Simon and McIntosh model and suggest that the water molecules in the head group region contribute most to the membrane dipole potential.

Dielectric Properties of the Membrane–Water Interface.

For the dielectric susceptibility near the lipid head group–water interface and near the ester groups we determined values around 30 and 10, respectively. These values are in agreement with experiments on PC and PS membranes.⁶¹ The susceptibility varies slowly in the lipid head group–water interface and varies rapidly in the ester group region. Due to limitations of the model used, the susceptibility in the lipid hydrocarbon region can not

be calculated. Calculation of the susceptibility in the hydrocarbon region would require us to implement an all-hydrogen-atom model and include atomic polarization effects in the force field. We expect that the electrostatic potential profile and the susceptibility profile obtained in this study can be incorporated, with easy modifications, into mesoscopic continuous medium descriptions of membrane transport properties.

Membrane Surface Charge Distributions. It is rather clear from this and other molecular dynamics studies that the Marčelja–Radic model³⁶ originally proposed to explain the membrane hydration force is over simplified. Not only is the thickness of the interface non-negligible but the charge distribution on the membrane surface is also inhomogeneous, as illustrated in Figure 11. Long-range correlations in surface charge densities are found for DLPE and POPC membranes. No significant difference is observed in the correlation function of surface charge densities between DLPE and POPC membranes despite the fact that hydrogen bonding between DLPE lipid head groups is also significant and differs from that found in the POPC membrane. Recent studies on hydrophobic surfaces⁹⁶ suggest that the surface charge distributions induce long-range attractive forces between these surfaces. Whether or not the fluctuation of the surface charge distribution indeed contributes to the membrane hydration force and whether or not the difference in the hydration of PE and PC membranes could be explained by the model of Kornyshev and Leikin⁴⁵ remain to be a subject of further studies.

It should also be kept in mind that the membranes simulated in this study and in our previous study¹² are highly ordered when constructed, and the simulation times (~200 ps) are rather short compared to the time needed for lipids to exchange places (~10 ns) and relax. The calculated correlation function of surface charge densities presented in Figure 12 exhibits some correlation between the two membrane leaflets and might be due to the fact that the initial distributions of lipid molecules in the two membrane leaflets were chosen too similar and did not relax completely. Further studies with membranes constructed in a more random way (such as starting from random positions using conformations obtained from Brownian dynamics²⁷) are necessary to obtain more reliable data on membrane surface charge distributions.

Effects of Employing a Cutoff Scheme in MD Simulation.

Our study demonstrates the strong influence of long-range Coulombic interactions on the electrical properties of membrane–water systems. A cutoff of the Coulombic forces has a significant effect on water polarization and causes an overestimate of the membrane dipole potential, particularly the potential due to hydration. Our conclusions are in agreement with a recent study⁹⁷ on a DMPC membrane bilayer–water system. In the studies of this system,^{97,98} it was further shown that the dynamic properties as well as the hydrogen-bonding properties of the water molecules are also affected when a short cutoff radius is used for Coulombic forces. From this study and other results in refs 97 and 98 one expects that long-range Coulombic interactions should also play a role for membrane–protein interactions, especially, when the protein or the membrane lipids are charged, such as in case of phospholipase A₂–membrane⁹⁹ or annexin–membrane¹⁰⁰ interactions.

Acknowledgment. We thank Andreas Windemuth for helping us in using the program MD and Helmut Heller for discussions on some technical parts of the simulation. Professor V. A. Parsegian has suggested to us to analyze the membrane surface charge distribution. The research and the calculations for this paper were carried out at the Resource for Concurrent Biological Computing funded by the National Institutes of

Health (P41RRO5969). This work was also supported by the National Science Foundation (ASC93-18159). Some simulations were accomplished on a Cray 2 computer operated by the National Center for Supercomputing Applications funded by the National Science Foundation.

References and Notes

- (1) Cevc, G.; Marsh, D. *Phospholipid Bilayers: Physical Principles and Models*; John Wiley & Sons: New York, 1987.
- (2) Brasseur, R., Ed. *Molecular description of biological membranes by computer aided conformational analysis*; CRC Press: Boca Raton, FL, 1990; Vols. 1 and 2.
- (3) Silver, B. L. *The Physical Chemistry of Membranes: an Introduction to the Structure and Dynamics of Biological Membranes*; Allen & Unwin and The Solomon Press; Publisher Creative Services Inc.: Jamaica, New York, 1985.
- (4) Gennis, R. B. *Biomembranes: Molecular Structure and Function*; Springer-Verlag: New York, 1989.
- (5) Lipowsky, R. *Nature* **1991**, *349*, 475.
- (6) Pullman, A., Ed. *Membrane proteins: structures, interactions and models*; Kluwer Academic Publishers: The Netherlands, 1992.
- (7) Peterson, N.; Chan, S. *Biochemistry* **1977**, *16*, 2657.
- (8) Pastor, R. W.; Venable, R. M.; Karplus, M.; Szabo, A. J. *Chem. Phys.* **1988**, *89*, 1128.
- (9) Speyer, J.; Weber, R.; Gupta, S. D.; Griffin, R. *Biochemistry* **1989**, *28*, 9569.
- (10) Qiu, X.; Pidgeon, C. J. *Phys. Chem.*, in press.
- (11) Rommel, E.; Noack, F.; Meier, P.; Kothe, G. J. *Phys. Chem.* **1988**, *92*, 9569.
- (12) Heller, H.; Schaefer, M.; Schulten, K. J. *Phys. Chem.* **1993**, *97*, 8343.
- (13) Board, J. A., Jr.; Causey, J. W.; Leathrum, J. F., Jr.; Windemuth, A.; Schulten, K. *Chem. Phys. Lett.* **1992**, *198*, 89.
- (14) Marčelja, S. *Nature* **1973**, *241*, 451.
- (15) Scott, H. *Biochim. Biophys. Acta* **1977**, *469*, 264.
- (16) Georgallas, A.; Pink, D. J. *Colloid. Interface Sci.* **1982**, *89*, 107.
- (17) Engelmann, A.; Llanos, C.; Nyholm, P.; Tapla, O.; Pascher, I. J. *Mol. Struct. (THEOCHEM)* **1987**, *151*, 81.
- (18) Scot, H.; Kalaskar, S. *Biochemistry* **1989**, *328*, 3687.
- (19) Pastor, R. W.; Venable, R. M.; Karplus, M. J. *Chem. Phys.* **1988**, *89*, 1112.
- (20) Loof, H. d.; Harvey, S. C.; Segrest, J. P.; Pastor, R. W. *Biochemistry* **1991**, *30*, 2099.
- (21) Ploeg, P. v. d.; Berendsen, H. J. C. J. *Chem. Phys.* **1982**, *76*, 3271.
- (22) Ploeg, P. v. d.; Berendsen, H. J. C. J. *Mol. Phys.* **1983**, *49*, 233.
- (23) Egberts, E.; Berendsen, H. J. C. J. *Chem. Phys.* **1988**, *89*, 3718.
- (24) Raghavan, K.; Reddy, M. R.; Berkowitz, M. L. *Langmuir* **1992**, *8*, 233.
- (25) Damodaran, K. V.; Kenneth M. Merz, J.; Gaber, B. P. *Biochemistry* **1992**, *31*, 7656.
- (26) Marrink, S.-J.; Berkowitz, M.; Berendsen, H. Manuscript.
- (27) Pastor, R.; Venable, R. Molecular and stochastic dynamics simulation of lipid molecules. In *Computer simulation of biomolecular systems: theoretical and experimental applications*; Gunsteren, W. v., Weiner, P., Wilkinson, A., Eds.; 1993.
- (28) Venable, R.; Zhang, Y.; Hardy, B. J.; Pastor, R. *Science* **1993**, *262*, 223.
- (29) Stouch, T. R. *Mol. Simul.* **1993**, *10*, 335.
- (30) Hitchcock, P. B.; Mason, R.; Thomas, K. M.; Shipley, G. G. *Proc. Natl. Acad. Sci. U.S.A.* **1974**, *71*, 3036.
- (31) Elder, M.; Hitchcock, P.; Mason, R.; Shipley, G. G. *Proc. R. Soc. London A (Math. Phys. Sci.)* **1977**, *354*, 157.
- (32) Pearson, R. H.; Pascher, I. *Nature* **1979**, *281*, 499.
- (33) McIntosh, T. J.; Simon, S. A. *Biochemistry* **1986**, *25*, 4948.
- (34) Rand, R. P.; Parsegian, V. A. *Biochim. Biophys. Acta* **1989**, *988*, 351.
- (35) Cevc, G.; Marsh, D. *Biophys. J.* **1985**, *47*, 21.
- (36) Marčelja, S.; Radic, N. *Chem. Phys. Lett.* **1976**, *42*, 129.
- (37) Simon, S. A.; McIntosh, T. J. *Proc. Natl. Acad. Sci. U.S.A.* **1989**, *86*, 9263.
- (38) Belaya, M.; Feigel'man, M.; Levadny, V. *Chem. Phys. Lett.* **1986**, *126*, 361.
- (39) Dzhevakhidze, P.; Kornyshev, A.; Levadny, V. *Phys. Lett. A* **1986**, *118*, 203.
- (40) Kjellander, R.; Marčelja, S. *Chem. Scr.* **1985**, *25*, 73.
- (41) Berkowitz, M. L.; Raghavan, K. *Langmuir* **1991**, *7*, 1042.
- (42) Cevc, G. J. *Chem. Soc., Faraday Trans.* **1991**, *87*, 2733.
- (43) Israelachvili, J. N.; Wennerström, H. *Langmuir* **1990**, *6*, 873.
- (44) Israelachvili, J. N.; Wennerström, H. J. *Phys. Chem.* **1992**, *96*, 520.
- (45) Kornyshev, A.; Leikin, S. *Phys. Rev. A* **1989**, *40*, 6431.
- (46) Rand, R.; Fuller, N.; Parsegian, V.; Rau, D. *Biochemistry* **1988**, *27*, 7711.
- (47) Liberman, Y. A.; Toplay, V. *Biophysics* **1969**, *14*, 477.
- (48) LeBlanc, O. *Biophys. J.* **1970**, *14*, 94a (Abstr.).
- (49) Flewelling, R.; Hubbell, W. *Biophys. J.* **1986**, *49*, 531.
- (50) Haydon, D.; Hladky, S. Q. *Rev. Biophys.* **1972**, *5*, 187.
- (51) Bangham, A. D.; Papahadjopoulos, D. *Biochim. Biophys. Acta* **1966**, *126*, 181.
- (52) Papahadjopoulos, D. *Biochim. Biophys. Acta* **1968**, *163*, 240.
- (53) McLaughlin, S. Electrostatic Potentials at membrane-solution interfaces. In *Current topics in membranes and transport*; Bronner, F., Kleinzeller, A., Eds.; Academic Press: New York, 1977; Vol. 9, p 71.
- (54) Honig, B. H.; Hubbell, W. L.; Flewelling, R. F. *Ann. Rev. Biophys. Chem.* **1986**, *15*, 163.
- (55) Paltauf, F.; Hauser, H.; Phillips, M. *Biochim. Biophys. Acta* **1971**, *249*, 539.
- (56) Cadenhead, D.; Bean, K. *Biochim. Biophys. Acta* **1972**, *290*, 43.
- (57) Gawrisch, K.; Ruston, D.; Zimmerberg, J.; Parsegian, V.; Rand, R.; Fuller, N. *Biophys. J.* **1992**, *61*, 1213.
- (58) Zheng, C.; Vanderkooi, G. *Biophys. J.* **1992**, *63*, 935.
- (59) Wang, J.; Pullman, A. *Biochim. Biophys. Acta* **1990**, *1024*, 10.
- (60) Chiu, S.-W.; Gulukota, K.; Jacobsen, E. Computational approaches in understanding the ion channel-lipid system. In *Membrane proteins: structures, interactions and models*; Pullman, A., Ed.; Kluwer Academic Publishers: The Netherlands, 1992; p 315.
- (61) Lelkes, P.; Miller, I. J. *Membrane Biol.* **1980**, *52*, 1.
- (62) Cevc, G.; Watts, A.; Marsh, D. *Biochemistry* **1981**, *20*, 4955.
- (63) Ashcroft, R.; Coster, H.; Smith, J. *Biochim. Biophys. Acta* **1981**, *643*, 191.
- (64) Jain, M.; Egmond, M.; Verheij, H.; Apitz-Castro, R.; Dijkman, R.; Haas, G. d. *Biochim. Biophys. Acta* **1982**, *688*, 341.
- (65) Watanabe, K.; Ferrario, M.; Klein, M. L. J. *Phys. Chem.* **1988**, *92*, 819.
- (66) Darden, T.; York, D.; Pedersen, L. J. *Chem. Phys.* **1993**, *98*, 10089.
- (67) York, D.; Darden, T.; Pedersen, L. J. *Chem. Phys.* **1993**, *98*, 8345.
- (68) Berkowitz, M.; McCammon, J. A. *Chem. Phys. Lett.* **1982**, *90*, 215.
- (69) Brooks, C. L., III; Brünger, A.; Karplus, M. *Biopolymers* **1985**, *24*, 843.
- (70) Blume, A. *Biochemistry* **1983**, *22*, 5436.
- (71) Windemuth, A. Dynamiksimulation von Makromolekülen. Master's thesis, Technical University of Munich, Physics Department, T 30, James-Frank-Street, D-8046 Garching/Munich, August 1988.
- (72) Windemuth, A.; Schulten, K. *Mol. Simul.* **1991**, *5*, 353.
- (73) Brünger, A. T. X-PLOR, Version 3.1; A System for X-ray Crystallography and NMR; The Howard Hughes Medical Institute and Department of Molecular Biophysics and Biochemistry, Yale University, 1992.
- (74) Brooks, B. R.; Bruccoleri, R. E.; Olafson, B. D.; States, D. J.; Swaminathan, S.; Karplus, M. J. *Comput. Chem.* **1983**, *4*, 187.
- (75) Greengard, L.; Rohklin, V. J. *Comput. Phys.* **1987**, *73*, 325.
- (76) Grubmüller, H.; Heller, H.; Windemuth, A.; Schulten, K. *Mol. Simul.* **1991**, *6*, 121.
- (77) Kubo, R. J. *Phys. Chem. Jpn.* **1957**, *12*, 570.
- (78) Glarum, S. H. J. *Chem. Phys.* **1960**, *33*, 1371.
- (79) Neumann, M.; Steinhauser, O.; Pawley, G. S. *Mol. Phys.* **1984**, *52*, 97.
- (80) Neumann, M. J. *Chem. Phys.* **1985**, *82*, 5663.
- (81) Neumann, M. J. *Chem. Phys.* **1986**, *82*, 1567.
- (82) King, G.; Lee, F.; Warshel, A. J. *Chem. Phys.* **1991**, *95*, 4366.
- (83) Seelig, A.; Seelig, J. *Biochemistry* **1974**, *13*, 4839.
- (84) Wiener, M. C.; White, S. H. *Biophys. J.* **1992**, *61*, 428.
- (85) Seddon, J.; Cevc, G.; Kaye, R.; Marsh, D. *Biochemistry* **1984**, *23*, 2634.
- (86) Lee, C.; McCammon, J.; Rossky, P. J. *Chem. Phys.* **1984**, *80*, 4448.
- (87) Latorre, R.; Hall, H. E. *Nature* **1976**, *264*, 361.
- (88) King, G.; Warshel, A. J. *Chem. Phys.* **1989**, *91*, 3647.
- (89) Damodaran, K.; Merz, K. J. *Langmuir* **1993**, *9*, 1179.
- (90) Parks, T. P.; Lukas, S.; Hoffman, A. F. Purification and characterization of a phospholipase A₂ from human osteoarthritic synovial fluid. In *Phospholipase A₂*; Wong, P. Y. K., Dennis, E. A., Eds.; Plenum Press: New York, 1990; p 55.
- (91) Reymolds, L. J.; Hughes, L. L.; Dennis, E. A. *Anal. Biochem.* **1992**, *204*, 190.
- (92) Warshel, A.; Russell, S. T. Q. *Rev. Biophys.* **1984**, *17*, 283.
- (93) Russell, S. T.; Warshel, A. J. *Mol. Biol.* **1985**, *185*, 389.
- (94) Smaby, J.; Brockman, H. *Biophys. J.* **1990**, *58*, 195.
- (95) Simon, S.; McIntosh, T.; Magid, A.; Needham, D. *Biophys. J.* **1992**, *61*, 786.
- (96) Tsao, Y.-H.; Evans, D. F.; Wennerström, H. *Science* **1993**, *262*, 547.
- (97) Alper, H. E.; Bassolino, D.; Stouch, T. R. J. *Chem. Soc.* **1993**, *98*, 9798.
- (98) Alper, H. E.; Bassolino, D.; Stouch, T. R. J. *Chem. Soc.* **1993**, *99*, 5547.
- (99) Ramikrez, F.; Jain, M. K. *Proteins* **1991**, *9*, 229.
- (100) Huber, R.; Berendes, R.; Burger, A. J. *Mol. Biol.* **1992**, *223*, 683.